Elongational flow birefringence of poly(styrene sulphonate)

R. S. Farinato
American Cyanamid Co., 1937 W. Main St., Stamford, CT 06904, USA
(Received 19 December 1986; accepted 13 May 1987)

The elongational flow birefringence of aqueous poly(styrene sodium sulphonate) solutions has been measured in a crossed-slot flow cell. The relaxation times calculated from the onset of birefringence were significantly longer than relaxation times determined from intrinsic viscosity measurements or reported for transient electric birefringence measurements. Direct observation of the flow birefringence patterns showed a more complex pattern than expected for simple non-interacting flexible polymers. A molecular connectedness of the flow-elongated polymers, first described by Odell *et al.*[1], was the most plausible explanation for the longer relaxation times, even for polymer concentrations well below the overlap concentration.

(Keywords: elongational flow birefringence; relaxation time; poly(styrene sodium sulphonate))

INTRODUCTION

Elongational flow birefringence measurements of polymer solutions can yield several types of information about the polymer, the flow field and the interaction of the two. For example, Keller and Odell[2] have described methods for calculating the relaxation times of both flexible and rigid macromolecules from the critical onset strain rate and the slope of the birefringence vs. strain rate curve, respectively. For dilute solutions these relaxation times are conveniently related to the rotational diffusion times of the macromolecules and hence their molecular weights under the assumption of an appropriate hydrodynamic model for the polymer. Keller and Odell[2] have also shown that for flexible macromolecules the first derivative of the birefringence vs. strain rate curve with respect to strain rate is proportional to the molecular weight distribution of the polymer. In the case where the flow field is sufficiently strong to achieve complete elongation and orientation of the macromolecule without causing turbulence, the optical anisotropy of the chain units can be calculated from the saturation value of the birefringence. This optical anisotropy can be compared with those determined from electric birefringence and polarized light scattering measurements.

Miles *et al.*[3] made a comprehensive study of the conformational relaxation times of sodium poly(styrene sulphonate) in aqueous solutions over a range of ionic strengths using elongational flow birefringence. They demonstrated a substantial decrease (greater than two orders of magnitude) in the relaxation time of this macromolecule as the ionic strength was increased to 0.06 M with sodium counterions. However, as shown in this paper, a comparison between these relaxation times from elongational flow birefringence and those calculated from intrinsic viscosity or transient electric birefringence data (see discussion below) showed substantial differences in the low ionic strength regime. The relaxation times from elongational flow birefringence were approximately two orders of magnitude larger than from either of the other two methods, which are within a factor of two of each other. The work reported in this paper tries to shed light on these differences.

In addition to quantitative determinations of the flow induced birefringence in polymer solutions, visualizations of the birefringent region can also yield valuable information. In this work, the resultant patterns of the elongationally stressed fluid between (nearly) crossed polarizing optics graphically demonstrated the flow field and its interaction with the dissolved polymer molecules. The birefringence patterns generated as a function of flow rate can be diagnostic for qualitative aspects of the polymer dynamics. For example, at low polymer concentrations flexible polymers would generally be expected to exhibit a thin birefringent line centred on the exit flow channels while rigid polymers would normally be expected to result in a more diffuse birefringent region. Odell *et al.*[1] have shown in their pioneering work that the elongational flow birefringence pattern can also be used to assess the molecular connectedness of transient networks of polymers in the semidilute regime. The birefringence patterns in such a case are more complex, as we will see below.

EXPERIMENTAL

For a collection of randomly oriented polymers in solution the bulk medium will be optically isotropic even though the polymers themselves might be highly anisotropic. One way of displaying this intrinsic anisotropic nature is by using an anisotropic force field such as occurs in elongational flow. Flexible molecules in such a hydrodynamic field will be stretched when the elongation rate is above a critical value. These elongated macromolecules, as well as any inherently stiff polymers, will then orient in the flow. This process can be monitored using the optical birefringence generated in the bulk solution. For dilute and semidilute polymer solutions typical magnitudes of the birefringence (refractive index difference between light polarized parallel and perpendicular to the elongation axis) produced in strong

0032-3861/88/010160-08$03.00

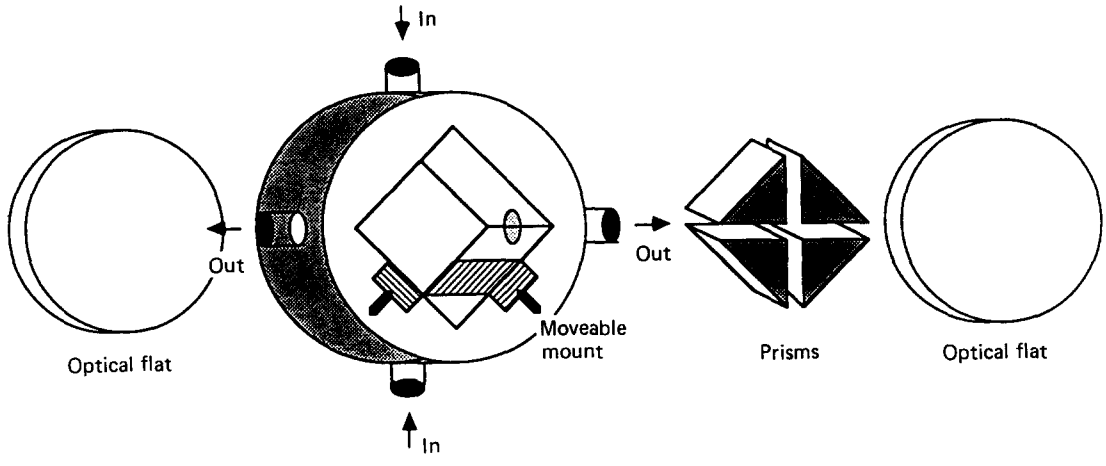

Figure 1 Elongational flow cell. Four 1 in × 1 in prisms are held ~2 mm apart in a holder and are sandwiched between optical flats. Moveable mounts provide for slot width adjustment and alignment

elongational flows range from 10^{-9} to 10^{-6}. This range is measurable with conventional polarimetry techniques (Azzam and Bashara[4]; Fredericq and Houssier[5]).

Flow cell

The flow geometry used was a crossed slot configuration which produced a nearly planar elongational flow near the region of the cross (except for some shear near the stationary walls) when fluid was pushed through two opposing slots and removed through the other two opposing slots. This type of flow field is very efficient for stretching and orienting macromolecules (Leal *et al.*[6]; Hinch[7]) and has been used routinely in the past (Keller and Odell[2]; Cressely *et al.*[8]; Lyazid *et al.*[9]).

The surfaces confining the flow in the observation region were 1 in × 1 in optical quality prism faces held 2 mm apart by a polyacetal (Delrin) holder and sandwiched between $\frac{1}{4}$ in thick optical flats (*Figure 1*). The optical flats were adjusted to be parallel with one another using front surface reflections of a 5 mW He–Ne laser (Hughes) beam. All other fittings were of polyacetal or nylon. All the glass surfaces in contact with fluid were made hydrophobic by dipping them in Nyebar (William F. Nye, Inc., New Bedford, MA), which is a solution of poly(1,1-dihydropentadecafluorooctyl methacrylate) in a fluorocarbon solvent. All interfaces were sealed with either a silicone elastic (Kerr Syringe Elasticon; Sybron/Kerr, Romulus, MI) or an artist's adhesive putty (Fun-Tak; Roberts Consolidated Ind., City of Industry, CA). Pulseless flow into the cell was from a helium pressurized stainless steel reservoir (Amicon) through polyethylene tubing. The flow rate was controlled by using a fixed gas pressure and adjusting a valve at the exit. In this configuration polymer solutions were passed through the flow cell only once to avoid using hydrodynamically degraded materials. The flow rate was monitored gravimetrically. The pressure drop across the flow cell was measured using either a 1 or 10 psi variable reluctance differential pressure transducer (Validyne DP15). For each data point the transmitted light intensity was recorded under steady state conditions of flow.

Flow induced birefringence

The flow cell and optical components were arranged on an optical rail (*Figure 2a*). For quantitative measurements a 5 mW He–Ne laser light source

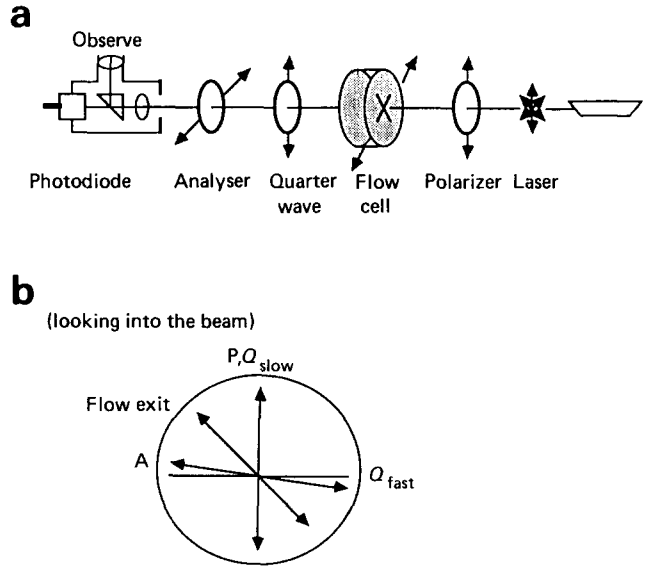

Figure 2 (a) Optics for elongational flow birefringence. (b) Optical axes of elements: polarizer (P) and quarter wave plate slow (Q_{slow}) axes are coincident; flow cell exit (FC) at 45° to P; analyser (A) is slightly off crossed position by an angle α

(632.8 nm) was used unfocused. Measuring angles from the vertical, the beam passed successively through a polarizer oriented vertically ($P=0°$), the flow cell with exit flow axis (FC) at 45°C, a mica quarter wave plate with its ordinary (slow) axis oriented vertically ($Q=0°$), an analyser oriented at or near the horizontal ($A=90°$), and finally into a silicon photodiode detector (United Detector Technologies, PIN-10DF with a 101C amplifier). All angles were measured viewing from the detector into the light source (*Figure 2b*) with counterclockwise rotations being positive (+). The polarizing elements were mounted dichroic sheets (Oriel) with an extinction coefficient of 2×10^{-4} as stated by the manufacturer. The quarter wave plate was a mica sheet (negative retardation; $n_e < n_0$) from Oriel, optimized for 632.8 nm light. In the flow visualization experiments the laser light source was replaced with either a focused tungsten lamp or a high intensity strobe lamp (Speedtron), and the detector was replaced with either a video recording unit (Sony WV 555B camera, Panasonic NV 9240 video cassette recorder, Panasonic BTS 1300N

monitor) or a 35 mm camera (Nikon F3 with a 200 mm lens) respectively. Videotape recordings were useful in studying the details of the flow birefringence patterns.

To determine the sign of the birefringence the analyser was turned slightly off the crossed position by an angular amount α in the direction of the polarizer (i.e. $A = 90° - \alpha$). For our experimental configuration and small positive values of α (i.e. $A < 90°$), if the transmitted light intensity decreased for small amounts of elongation of the polymer solution, then the birefringence was negative. If the light intensity increased under the same conditions, then the birefringence was positive (Fredericq and Houssier[5]). The converse was true for small negative values of α (i.e. $A > 90°$). Checking the birefringence patterns visually with the analyser on both sides of the crossed position (usually $\pm 5°$) to see that one pattern was the inverse of the other (i.e. dark birefringent regions became light and vice versa when the analyser was turned to other side of crossed position) was a good method for substantiating a true birefringence and to distinguish it from refractive index gradient effects (concentration or thermal gradients).

We followed the method of Fredericq and Houssier[5] to determine the birefringence from the raw data. Our optical configuration resulted in a birefringence induced transmitted light intensity which was equivalent to one of their configurations with a quarter wave plate (loc. cit., pp. 90–92). This was true even though the Mueller matrices for the two configurations were not identical. A more detailed analysis is presented in Appendix 1.

The stray light constant, K_{SL}, which is a measure of the optical quality of the apparatus, was determined without the flow cell in place. In the analysis below, the primed variables refer to the optics without the flow cell in place; the unprimed variables are for measurements with the flow cell in place. The transmitted light intensity, $I'(\alpha)$, for the analyser α degrees off the crossed position was measured as a function of $\sin^2\alpha$. The intercept at $\sin^2\alpha = 0$ gave the stray light intensity without the cell, $I'(\mathrm{SL})$. The stray light constant was then given by:

$$K_{SL} = \frac{I'(\mathrm{SL})\sin^2\alpha}{I'(\alpha) - I'(\mathrm{SL})} \tag{1}$$

and was calculated from the slope of $I'(\alpha)$ vs. $\sin^2\alpha$. For our apparatus K_{SL} was $\sim 10^{-5}$. This could easily be improved by using better polarizing optics for more accurate studies of the magnitude of the birefringence. The residual retardation, δ_0, of the flow cell was determined implicitly from:

$$I(\alpha) - I(\mathrm{SL}) = \frac{I(\mathrm{SL})[1 - \cos(2\alpha)\cos(\delta_0)]}{2K_{SL}} \tag{2}$$

where the stray light intensity with the cell in place was calculated from:

$$I(\mathrm{SL}) = \frac{I(\alpha)K_{SL}}{\sin^2\alpha + K_{SL}} \tag{3}$$

This procedure allowed the separation of effects due to the optics and residual birefringence in the flow cell. Typical values of δ_0 were several tenths of a degree (a few hundredths of a radian). The actual birefringence retardation, δ, due to the flowing polymer solution was then determined implicitly from the transmitted light intensity, $I(\delta)$, under flow conditions.

$$\frac{I(\delta) - I(\alpha)}{I(\alpha) - I(\mathrm{SL})} = \frac{\cos(2\alpha + \delta_0) - \cos(2\alpha + \delta + \delta_0)}{2\sin^2(\alpha + \delta_0/2)} \tag{4}$$

The birefringence, Δn, was calculated from the retardation

$$\Delta n = \frac{W\delta}{2\pi L} \tag{5}$$

where light of wavelength W had passed through a cell of path length L. Note that for small values of the retardation and negligible values of both the residual retardation and the stray light intensity, equation (4) reduces to:

$$\frac{I(\delta)}{I(\alpha)} \approx \frac{\delta}{\tan\alpha} \tag{6}$$

Hence, for such conditions the retardation (and the birefringence) was proportional to the transmitted light intensity. Recall that this was for the case of having a quarter wave plate in the optical train. Without this optical element and for similar conditions as above, the birefringence would have been proportional to the square root of the transmitted intensity and the sign of the birefringence would have been indeterminate.

Polymer solutions

All polymers were dissolved in water purified first by deionization, then reverse osmosis filtration (MilliQ System) and finally by filtration through a 0.2 μm Nuclepore filter. Stock solutions at either 0.2 or 1.0 wt% were prepared by rolling the solutions at least overnight in glass bottles with polyethylene lined caps. The stock solutions were then filtered slowly (~ 0.1 litre h^{-1}) through 8 μm Nuclepore filters. Dilutions were made with the purified water and the solutions were equilibrated with rolling for at least another day. For solutions containing glycerol, the glycerol (Aldrich 99+ %) was prefiltered (8 μm Nuclepore) before dissolving.

Poly(styrene sodium sulphonate) (NaPSS) was obtained from Scientific Polymer Products. The manufacturer reported a nominal molecular weight of 0.5×10^6 and a degree of sulphonation of 100%. The intrinsic viscosity of this material in pure water (sample not dialysed), determined from four-bulb capillary viscometer data extrapolated to zero shear rate, was 9.5 dl g^{-1}. A 1.0 wt% stock solution had a pH of 6.2.

RESULTS

All solutions (aqueous NaPSS with and without glycerol) over the concentration range 0.02–0.4 wt% displayed a critical onset strain rate, $\dot{\varepsilon}_c$, for birefringence. *Figure 3* shows a typical pair of experimental curves for the transmitted light intensity and the pressure drop across the flow cell for 0.2 wt% NaPSS in 40% glycerol. *Figure 4* shows the same data on an expanded scale to illustrate the onset of birefringence. Some of the relaxation times, τ_{fb}, calculated from $\dot{\varepsilon}_c$ values of NaPSS in water using the formula for flexible polymers (Keller and Odell[2]) are

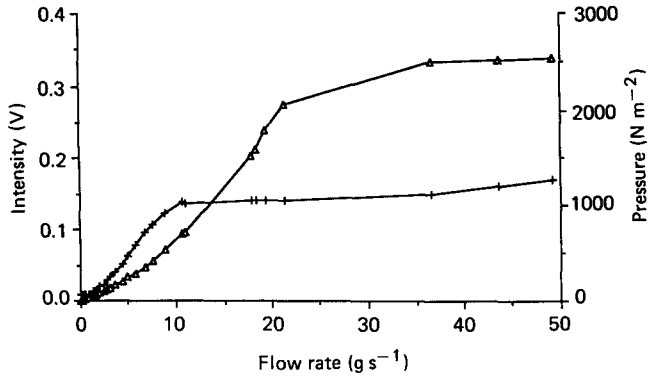

Figure 3 Transmitted light intensity (V) (+) and pressure drop (N m^{-2}) (△) across flow cell vs. mass flow rate (g s^{-1}) for 0.02 wt% NaPSS in 40% glycerol. Analyser is at 90° ($\alpha = 0°$) to the polarizer. Nominal elongation rate (s^{-1}) = 10 times mass flow rate (g s^{-1})

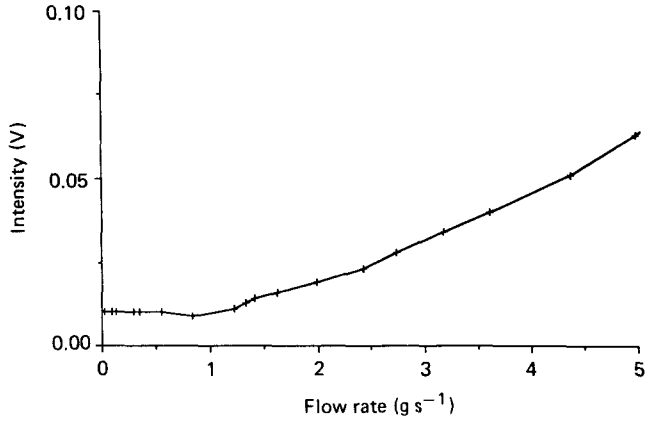

Figure 4 Transmitted light intensity (V) vs. mass flow rate (g s^{-1}) for 0.02 wt% NaPSS in 40% glycerol (same as *Figure 3* except on expanded scale). Analyser is at 90° ($\alpha = 0°$) to the polarizer. Note onset of birefringence at 1 g s^{-1} ($\dot{\varepsilon}_c = 10$ s^{-1})

shown in *Table 1*.

$$\tau_{fb} = 1/\dot{\varepsilon}_c \tag{7}$$

These were compared (*Table 1*) with other flow birefringence (Miles *et al.*[3]) and transient electric birefringence (τ_{eb}) relaxation data (Yamaoka and Ueda[10]; Wijmenga *et al.*[11]) from the literature, as well as the lowest normal mode Rouse relaxation time (τ_{iv}) calculated from the intrinsic viscosity, $[\eta]$.

$$\tau_{iv} = \frac{[\eta]\eta_s M}{A k_b T} \tag{8}$$

The additional variables above are the solution viscosity, η_s, the molecular weight of the polymer, M, the Avogadro number, A, the Boltzmann constant, k_b, and the absolute temperature, T. We also used equation (8) in combination with Mark–Houwink coefficients for NaPSS cited in the 'Polymer Handbook' (Brandup and Immergut[12]) to compute τ_{iv} for molecular weights equal to those used in the study of Miles *et al.*[3]

We were initially perplexed as to why the relaxation times from elongational flow birefringence for dilute aqueous poly(styrene sodium sulphonate) were more than an order of magnitude larger than expected from measurements using other techniques, in some cases on the same material. This was clarified by directly observing the birefringent region in the flow cell.

Figures 5a–5d show a sequence of flow induced birefringence patterns for 0.1% NaPSS in 40% glycerol at increasing flow rates. The results were qualitatively the same in aqueous and glycerol solutions of NaPSS. However, the lower viscosity of the aqueous solutions allowed inertial effects, which produced chaotic birefringence patterns, to set in at lower flow rates. Higher elongational strain rates before the jump to turbulent flow could be achieved in the glycerol solutions than in the aqueous solutions. The fact that the patterns in water and in glycerol were similar suggested that the diffuse birefringent region was probably not due to a charge related polymer expansion.

Even at strain rates just above $\dot{\varepsilon}_c$ it was evident that a composite birefringence pattern resulted: a thin birefringent line centred along the exit flow axis, indicative of a dilute flexible polymer solution, was surrounded by a diffuse birefringent region occupying most of the centre of the cell. Both of the features were negatively birefringent and were quite stable over time as long as the flow persisted. At slightly higher flow rates the central thin line gradually thickened as the flow rate increased, finally merging with the diffuse pattern which occupied most of the crossed region of the flow cell. This birefringent region extended a short way back into the entrance slots.

At any particular flow rate below a chaotic threshold the pattern was very stable. These global patterns were quite similar to the 'flare' patterns seen by Odell *et al.*[1] in an opposed jet apparatus for nonionic polystyrene and described for poly(styrene sulphonate), except that the patterns seen in this work were stable. One possible reason for the stability of the patterns in our experiments was the presence of the additional confining stationary walls in the crossed slot flow cell compared to the opposed jet configuration. As described by Odell *et al.*[1], these extensive birefringence patterns were a manifestation of the molecular connectedness of the elongated macromolecules, a transition to semidilute behaviour at mass concentrations of the polymer well below the overlap concentration under either quiescent or weak flow conditions. These patterns signalled the networking between these macromolecules under elongational flow at

Table 1 Comparison of polymer relaxation times in water

Polymer	$MW \times 10^{-6}$	$[\eta]$ (dl g^{-1})	c (g dl^{-1})	Relaxation times (ms) τ_{fb}	τ_{eb}	τ_{iv}
NaPSS	0.5	9.5	0.1	50		0.19
NaPSS[a]	0.3		0.015		0.035	
NaPSS[b]	0.69		0.1	15		0.2[c]
NaPSS[d]	0.59		0.06		0.051	
			0.73		0.14	

τ_{fb}, flow birefringence; τ_{eb}, electric birefringence; τ_{iv}, intrinsic viscosity

[a] Yamaoka, K. and Ueda, K. *Bull. Chem. Soc. Jpn.* 1983, **56**, 2390

[b] Miles, M. J., Tanaka, K. and Keller, A. *Polymer* 1983, **24**, 1081

[c] Calculated using extrapolated values of the Mark–Houwink coefficients found in Brandup and Immergut (1975); $K = 0.002$ ml g^{-1}; $a = 0.95$

[d] Wijmenga, S. S., van der Touw, F. and Mandel, M. *Polymer* 1985, **26** (*Commun.*) 172

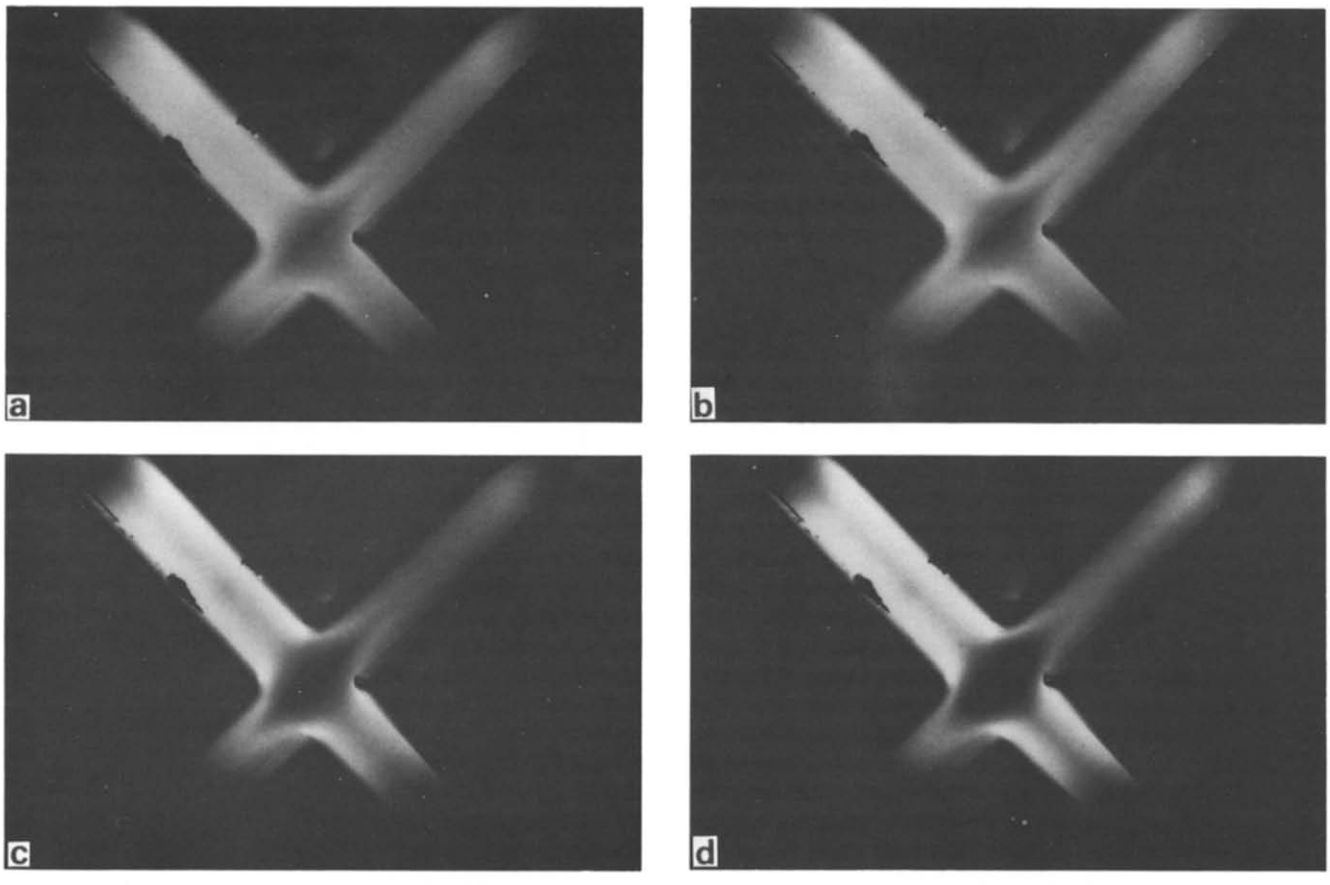

Figure 5 Flow induced birefringence from 0.1 wt % NaPSS in 40 % glycerol at room temperature. Slot width is 2 mm. Analyser is at 95° to the polarizer ($\alpha = -5°$), resulting in a light background. Negative birefringence appears dark. Flow is in from the upper right and lower left slots, and the flow exits through the upper left and lower right slots. Mass flow rates (nominal elongation rates) through cell are: (a) 5.5 (55); (b) 7.8 (78); (c) 10.7 (107); (d) 15.9 g s^{-1} (159 s^{-1})

polymer concentrations well below the traditional semidilute regime. In these experiments we saw the general behaviour described above even at the lowest concentration tested (0.02 wt %), which was approximately one-fifth of c^* ($=1/[\eta]$), an estimate of the overlap concentration from viscometric studies.

Observation of these flow birefringence patterns gave an indication of the reason for the discrepancies between relaxation times calculated from the flow birefringence onset and other methods such as transient electric birefringence and intrinsic viscosity. The low flow rate birefringence signal was not due solely to the behaviour of a dilute solution of flexible polymers upon which the relaxation time calculation was based. There were two possible contributions to this phenomenon. The global birefringence patterns were seen well below even a conservative estimate of the overlap concentration under quiescent conditions. However, as Odell *et al.*[1] have discussed and our data corroborated, networking can be significant at these concentrations. This would make the birefringence onset at a lower flow rate resulting in a longer calculated relaxation time. Another contribution to this earlier birefringence onset might have come from a significant population of naturally extended molecules or segments. These would have partially aligned at all flow rates and would have produced a broad birefringent region. However, the diffuse birefringent region observed was globular even at low flow rates and did not have the appearance of a thick line extending far down the exit slot as we have seen, for example, in xanthan (a stiff macromolecule; data unpublished). Excimer fluorescence data (Turro and Okubo[13]) on poly(styrene sodium sulphonate) in aqueous solution suggested that the pendant phenyl group correlations extended only over several adjacent monomer units and gave no indication of long stiff segments. These considerations made a stiff polymer contribution to the flow birefringence seem unlikely.

In addition to the dominant birefringence patterns in the centre of the flow cell, a weaker birefringent region along the inlet slot walls appeared after the onset of the central pattern and was seen to grow stronger with flow rate. The sign of the birefringence along the inlet walls was also negative. The magnitude of the wall birefringence increased with flow rate, but was always significantly less than the birefringence in the centre of the cell. A similar effect was seen in the exit channels in addition to the dominant central birefringence pattern. This wall birefringence was analogous to classical shear flow birefringence experiments. The greater efficiency of elongational flow fields for orienting macromolecules was graphically demonstrated in the side by side comparison of the magnitudes of the two effects in the same flow experiment.

The negative birefringence seen for NaPSS was in agreement with pulsed electric birefringence measurements in the literature (loc. cit.). The large optical polarizability perpendicular to the polymer chain

responsible for this negative birefringence was due largely to the phenyl substituents.

Inertial effects in these experiments limited the degree of macromolecular orientation achieved. The orientation function, Φ, as used in the electric birefringence literature (Fredericq and Houssier[5]) was used as a measure of the degree of orientation. It is essentially a ratio of the birefringence at one set of conditions to the birefringence, Δn_{sat}, at complete (saturation) orientation.

$$\Phi = \Delta n / \Delta n_{sat} \tag{9}$$

The values of $\Delta n_{sat}/c$ for poly(styrene sodium sulphonate) from electric birefringence vary by about a factor of two in the literature (Yamaoka and Ueda[10]; Tricot and Houssier[14]). Using this range we found the maximum Φ achieved in our flow cell before inertial effects set in was 1–2% for a 0.1% NaPSS in 40% glycerol sample and 1.5–3% for a 0.02% NaPSS in 40% glycerol sample. It should be noted that our experimental curves of transmitted light intensity vs. flow rate (see *Figure 3*) typically showed a plateau or a maximum. The values of the orientation function stated above correspond to these plateau or maximum signals. For the case of flexible macromolecules in these elongational flow experiments we cannot directly separate the extent of elongation from the extent of orientation. However, as was noted above, under similar flow conditions a stiff polymer (xanthan) achieved full orientation in the flow. This suggests that the poly(styrene sulphonate) was not completely oriented in these flows before turbulence set in, and that the onset of turbulence was responsible for the plateau or maximum in the data. Evidence for this was also seen in the pressure drop across the flow cell, which reached a plateau at the same flow rate as did the transmitted light intensity.

CONCLUSIONS

A comparison of aqueous poly(styrene sodium sulphonate) relaxation times from elongational flow birefringence, transient electric birefringence and intrinsic viscosity experiments showed the flow birefringence relaxation times at low polymer concentrations to be significantly longer than the others. Flow visualizations helped to establish that this difference was accompanied by a more complex flow birefringence pattern than expected for simple non-interacting flexible polymers. A molecular connectedness of the flow elongated polymers, first described by Odell *et al.*[1], was the most plausible explanation for the larger relaxation times, even for polymer concentrations well below the overlap concentration. The sign of the birefringence measured using elongational flow was negative, even in the composite birefringence patterns. This was in accord with electric birefringence measurements found in the literature.

ACKNOWLEDGEMENTS

The professional assistance of Bruce Hibbs is gratefully acknowledged in photographing the flow birefringence patterns. The clarifying discussions with Dr Wei Yen were greatly appreciated.

REFERENCES

1 Odell, J. A., Keller, A. and Miles, M. J. *Polymer* 1985, **26**, 1219
2 Keller, A. and Odell, J. A. *Colloid Polym. Sci.* 1985, **263**, 181
3 Miles, M. J., Tanaka, K. and Keller, A. *Polymer* 1983, **24**, 1081
4 Azzam, R. M. A. and Bashara, N. M. 'Ellipsometry and Polarized Light', North-Holland, 1977
5 Fredericq, E. and Houssier, C. 'Electric Dichroism and Electric Birefringence', Clarendon, 1973
6 Leal, L. G., Fuller, G. G. and Olbricht, W. L. *Prog. Astron. Aerosp.* (Ed. G. R. Hough) 1980, **72**, 351
7 Hinch, E. J. *Phys. Fluids* 1977, **20**(10), Pt. 11, S22–S30
8 Cressely, R., Hocquart, R., Decruppe, J.-P. and Wydro, T. in Proc. Microsymp. 27th Macromol. 1985, pp. 507–510
9 Lyazid, A., Scrivener, O. and Teitgen, R. in 'Rheology', (Eds. G. Astarita, G. Marrucci and L. Nicolais), 1980, Vol. 2
10 Yamaoka, K. and Ueda, K. *Bull. Chem. Soc. Jpn.* 1983, **56**, 2390
11 Wijmenga, S. S., van der Touw, F. and Mandel, M. *Polymer* 1985, **26** (*Commun.*), 172–175
12 Brandup, J. and Immergut, E. H. 'Polymer Handbook', 2nd edn., Wiley–Interscience, 1975
13 Turro, N. J. and Okubo, T. *J. Phys. Chem.* 1982, **86**, 1485
14 Tricot, M. and Houssier, C. *Macromolecules* 1982, **15**, 854
15 Mueller, H. *J. Opt. Soc. Am.* 1948, **38**, 661

APPENDIX 1

Mueller matrix analysis of elongational flow birefringence apparatus

The fate of the intensity and polarization of partially polarized quasi-monochromatic light propagating through an optical system consisting of depolarizing elements can be conveniently determined using the Mueller matrix formalism (Azzam and Bashara[4]; Mueller[15]). In this formalism the intensity and polarization state of a quasi-monochromatic transverse-electric (TE) light wave is described by its 4-component Stokes vector. Optical elements are modelled as 4×4 matrices which transform the Stokes vector of the incident wave into the Stokes vector of the output wave. The total effect of a series of optical elements can be computed as a single matrix transformation which is the matrix product of the individual Mueller matrices of the optical elements and rotation matrices describing reference frame rotations of the optical elements.

If an optical element is modelled by a Mueller matrix $\mathbf{M}$ and the defining axis of that element is rotated from the reference direction by β degrees (counterclockwise rotation when viewing into the beam propagation direction), the new Mueller matrix, $\mathbf{M}'$, is given by:

$$\mathbf{M}' = \mathbf{R}(-\beta)\mathbf{M}\mathbf{R}(\beta) \tag{A1}$$

Rotation matrices are of the form:

$$\mathbf{R}(\beta) = \begin{bmatrix} 1 & 0 & 0 & 0 \\ 0 & \cos 2\beta & \sin 2\beta & 0 \\ 0 & -\sin 2\beta & \cos 2\beta & 0 \\ 0 & 0 & 0 & 1 \end{bmatrix} \tag{A2}$$

The configuration of the elongational flow birefringence experiment described in this paper is shown in the diagram below as if we were looking from the detector

into the beam:

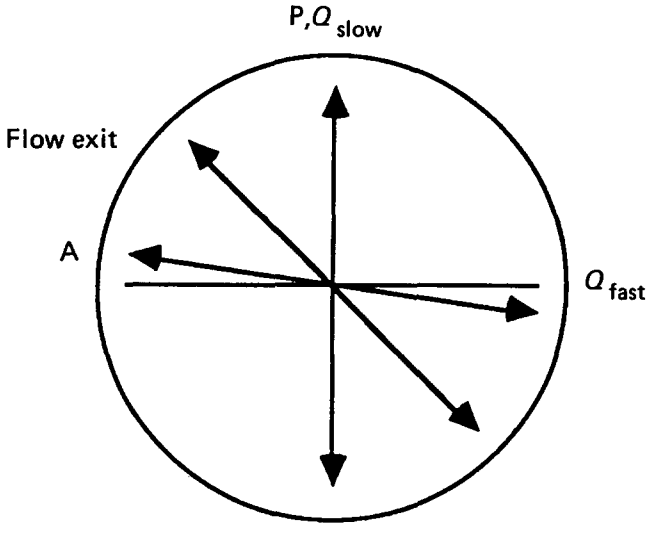

We chose as a reference the axis of the flow cell exits (FC) along which the polymer molecules would be stretched and oriented. This is equivalent to the electric field axis in electric birefringence experiments. An equivalent representation to the diagram above is:

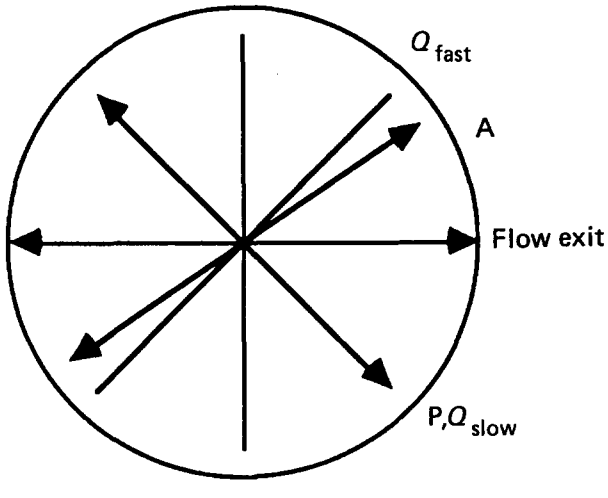

The Mueller matrix for the total configuration is given by:

$$\mathbf{M}_{tot} = \mathbf{M}'_a\mathbf{M}'_q\mathbf{M}'_\delta\mathbf{M}'_p \tag{A3}$$

where the first term in the product is for the analyser, the second term is for the quarter wave plate, the third term is for the birefringent medium in the flow cell, and the fourth term is for the polarizer. Using the Mueller matrices for standard optical elements as found in Azzam and Bashara[4] and applying the appropriate rotation matrices using FC as the reference we find for the above optical configuration the following Mueller matrices. For the analyser:

$$\mathbf{M}'_q = \mathbf{R}(-45)\mathbf{M}_{\delta=90}\mathbf{R}(45) \tag{A6}$$

$$\mathbf{M}'_a = 1/2\begin{bmatrix} 1 & \sin 2\alpha & \cos 2\alpha & 0 \\ \sin 2\alpha & \sin^2 2\alpha & \sin 2\alpha \cos 2\alpha & 0 \\ \cos 2\alpha & \sin 2\alpha \cos 2\alpha & \cos^2 2\alpha & 0 \\ 0 & 0 & 0 & 0 \end{bmatrix} \tag{A5}$$

the quarter wave plate:

$$\mathbf{M}'_q = \mathbf{R}(-45)\mathbf{M}_{\delta=90}\mathbf{R}(45) \tag{A6}$$

$$\mathbf{M}'_q = \begin{bmatrix} 1 & 0 & 0 & 0 \\ 0 & 0 & 0 & -1 \\ 0 & 0 & 1 & 0 \\ 0 & 1 & 0 & 0 \end{bmatrix} \tag{A7}$$

the flow cell (retardation $= \delta$):

$$\mathbf{M}'_\delta = \mathbf{M}_\delta \tag{A8}$$

$$\mathbf{M}'_\delta = \begin{bmatrix} 1 & 0 & 0 & 0 \\ 0 & 1 & 0 & 0 \\ 0 & 0 & \cos\delta & \sin\delta \\ 0 & 0 & -\sin\delta & \cos\delta \end{bmatrix} \tag{A9}$$

and the polarizer:

$$\mathbf{M}'_p = R(45)\mathbf{M}'_p\mathbf{R}(-45) \tag{A10}$$

$$\mathbf{M}'_p = 1/2\begin{bmatrix} 1 & 0 & -1 & 0 \\ 0 & 0 & 0 & 0 \\ -1 & 0 & 1 & 0 \\ 0 & 0 & 0 & 0 \end{bmatrix} \tag{A11}$$

The total Mueller matrix for the above configuration is:

$$\mathbf{M}_{tot} = \frac{[1-\cos(2\alpha-\delta)]}{4}\begin{bmatrix} 1 & 0 & -1 & 0 \\ \sin 2\alpha & 0 & -\sin 2\alpha & 0 \\ \cos 2\alpha & 0 & -\cos 2\alpha & 0 \\ 0 & 0 & 0 & 0 \end{bmatrix} \tag{A12}$$

The laser used in these experiments produced vertically polarized light. The transmitted light intensity, I_0, relative to the incident light intensity, I_i, is given by (Azzam and Bashara[4]):

$$\tau = I_0/I_i \tag{A13}$$

$$= m_{11} + P[m_{12}\cos 2\varepsilon \cos 2\theta + m_{13}\cos 2\varepsilon \sin 2\theta + m_{14}\sin 2\varepsilon]$$

where the m_{1i} are the first row elements of the composite Mueller matrix for the system, P is the degree of polarization, ε the ellipticity angle and θ the azimuth of the incident light. For a perfectly polarized (along the polarizer axis) laser: $P=1$, $\varepsilon=0$, $\theta=0$. The light transmission through the optical configuration described above would be:

$$\tau = \frac{1-\cos(2\alpha-\delta)}{4} \tag{A14}$$

Applying a similar analysis to the optical configuration with a quarter wave plate described by Fredericq and

Houssier[5]

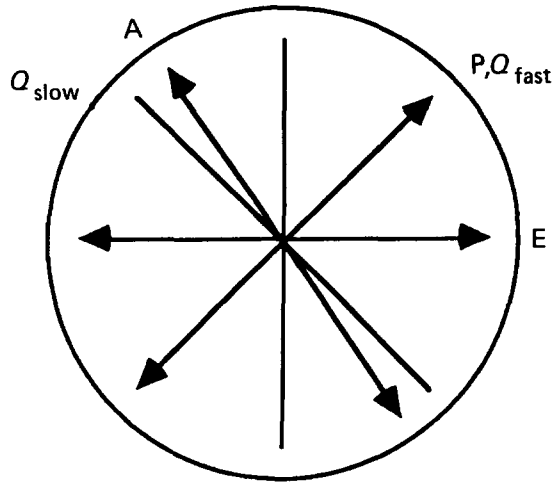

resulted in a Mueller matrix for the total configuration of:

$$\mathbf{M}_{tot}=\frac{[1-\cos(2\alpha-\delta)]}{4}\begin{bmatrix}1 & 0 & 1 & 0\\ -\sin 2\alpha & 0 & -\sin 2\alpha & 0\\ -\cos 2\alpha & 0 & -\cos 2\alpha & 0\\ 0 & 0 & 0 & 0\end{bmatrix} \quad \text{(A15)}$$

For the same incident polarized light beam as described above the relative transmitted light intensity through this optical configuration would also be given by equation (A14).

Therefore, for our purposes, while the two configurations described are not completely equivalent, in the elongational flow birefringence experiment described here the transmitted light intensities would be the same for both configurations.